

Parametric Chordal Sparsity for SDP-based Neural Network Verification

Anton Xue, Lars Lindemann, and Rajeev Alur

Abstract—Many future technologies rely on neural networks, but verifying the correctness of their behavior remains a major challenge. It is known that neural networks can be fragile in the presence of even small input perturbations, yielding unpredictable outputs. The verification of neural networks is therefore vital to their adoption, and a number of approaches have been proposed in recent years. In this paper we focus on semidefinite programming (SDP) based techniques for neural network verification, which are particularly attractive because they can encode expressive behaviors while ensuring a polynomial-time decision. Our starting point is the DeepSDP framework proposed by Fazlyab et al, which uses quadratic constraints to abstract the verification problem into a large-scale SDP. When the size of the neural network grows, however, solving this SDP quickly becomes intractable. Our key observation is that by leveraging *chordal sparsity* and specific parametrizations of DeepSDP, we can decompose the primary computational bottleneck of DeepSDP — a large linear matrix inequality (LMI) — into an equivalent collection of smaller LMIs. Our parametrization admits a tunable parameter, allowing us to trade-off efficiency and accuracy in the verification procedure. We call our formulation Chordal-DeepSDP, and provide experimental evaluation to show that it can: (1) effectively increase accuracy with the tunable parameter and (2) outperform DeepSDP on deeper networks.

I. INTRODUCTION

The success of neural networks is well documented in the literature for various applications, e.g., in Go [1], in handwritten character recognition [2], and in autonomous driving [3]. Neural networks are, however, notoriously opaque. The key challenges in analyzing their behavior are two-fold: first, one must appropriately model the nonlinear activation functions; second, the neural network may be very large. In addition, neural networks are often sensitive to input perturbations [4], [5], meaning that test-driven methods may insufficiently cover the input domain. It is hence often unclear what a neural network exactly learns, and how certain desirable properties can be verified. This is of particular concern in safety-critical applications like autonomous driving, where the lack of formal verification guarantees poses a serious barrier to adoption. In this work we focus on *safety verification*: given a neural network $f : \mathbb{R}^{n_1} \rightarrow \mathbb{R}^m$ and a specification $\mathcal{S} \subseteq \mathcal{X} \times \mathbb{R}^m$ where $\mathcal{X} \subseteq \mathbb{R}^{n_1}$ is the admissible input domain, does the neural network f satisfy \mathcal{S} ? In other words, is it the case that

$$(x, f(x)) \in \mathcal{S} \text{ for all } x \in \mathcal{X}?$$

Anton Xue and Rajeev Alur are with the Department of Computer and Information Science, University of Pennsylvania, PA, USA (email: antonxue@seas.upenn.edu and alur@seas.upenn.edu).

Lars Lindemann is with the Department of Electrical and Systems Engineering, University of Pennsylvania, PA, USA (email: larsl@seas.upenn.edu).

Our starting point is the DeepSDP verification framework presented in [6], with a focus on improving scalability. DeepSDP uses quadratic constraints to abstract nonlinear activation functions, yielding a convex relaxation of the safety verification problem as a large SDP. When the neural network grows larger, however, solving DeepSDP becomes intractable — thereby motivating our work.

We observe that although DeepSDP [6] itself does not exploit any sparsity to improve scalability, it was recently noted in [7] that a particular instantiation of DeepSDP for neural networks with ReLU activation functions admits *chordal sparsity* [8], [9], [10] in its LMI constraint — the key computational bottleneck. This insight allows the authors of [7] to then decompose and efficiently solve this version of DeepSDP. This approach improves scalability, but lacks two features critical to the original DeepSDP work. First, the formulation presented in [7] is the sparsest parametrization of DeepSDP using a restrictive abstraction of the activation function behavior — which cannot capture the interaction of neurons across nonadjacent layers. Moreover, this approach cannot verify specifications with input-output coupling, e.g. the L_2 gain κ of a network f posed as $\|f(x)\|^2 \leq \kappa\|x\|^2$.

In this work we present an alternative parametrization of DeepSDP that overcomes both limitations. We present a tunable parametrization of DeepSDP that leads to different levels of chordal sparsity, allowing us to trade-off sparsity and accuracy in the verification result. Importantly, our tunable parametrization allows us to recover a form similar to [7] as well as the original DeepSDP formulation at the extreme ends of the efficiency-accuracy spectrum. Furthermore, our approach retains the full expressive power of DeepSDP’s specifications, in particular the ability to encode arbitrary quadratic input-output specifications — a distinguishing feature of SDP-based neural network verification techniques. Particularly, our **contributions** are as follows:

- We propose the Chordal-DeepSDP method for SDP-based verification of neural networks with general activation functions. We particularly show that specific parametrizations of DeepSDP admit chordally sparse decompositions, allowing us to formulate the equivalent Chordal-DeepSDP problem using smaller constraints. The primary benefit is scalability, as the main computational bottleneck of DeepSDP — a large LMI — is now decomposed into an equivalent collection of smaller LMIs without incurring any accuracy loss.
- We present techniques for bolstering the accuracy and scalability of Chordal-DeepSDP. We show how additional constraints can further tighten the verification accuracy while retaining the same chordal decomposition

structure. Moreover, we observe that a second level of chordal decomposition is possible, allowing us to further accelerate the run time.

- We provide numerical evaluations to show the effectiveness of Chordal-DeepSDP. We show on a set of deep random networks that Chordal-DeepSDP outperforms DeepSDP in terms of efficiency without inducing conservatism. Our open source implementation is available at <https://github.com/AntonXue/nn-sdp>.

A. Related Work

The safety verification of neural networks has found broad interest over the past years and there have been various departures to address the problem [11], [12]. Great success was achieved with Reluplex [13], which is a specialized satisfiability modulo theories (SMT) based verification method that interleaves the simplex procedure with boolean satisfiability solving. While Reluplex only applies to feedforward neural networks with ReLU activation functions, the technique was extended to fully connected and convolutional neural networks with arbitrary piecewise-linear activation functions with Marabou [14]. Other works in SMT-based verification include [15], [16]. Related to SMT-solving has been the use of mixed-integer programming such as in [17], [18], [19]. These methods give accurate results for various types of neural networks and are in fact complete for ReLU activation functions, but they are fundamentally hard-to-solve combinatorial problems.

Another way of approaching safety verification is by reformulating it as a reachability problem, see e.g., [20], [21], [22], [23], [24], [25] which has been of particular interest for the safety verification of closed-loop dynamical systems [26]. While heuristics for reachability problems over dynamical systems exist, these methods are typically computationally expensive. Safety verification methods based on abstract interpretations [27], [28], [29], [22], [30] work by soundly over-approximating the input set into a convenient abstract domain, e.g. polytopes or zonotopes, and then propagating the abstracted representation through the network. Then, properties verified on the abstract output domain imply that the same properties hold on the original system. These approaches generally offer good scalability, but one must carefully choose good abstract domains and transformers to preserve accuracy.

Broadly related to this work is the idea to formulate neural network verification as a convex optimization problem. For scalability, linear approximations have been presented in [31], [32] where particularly [31] is amendable to parallelization via ADMM [33]. Techniques for interval analysis like β -CROWN [34] are also GPU-parallelizable. Further related are convex optimization-based techniques [35], which commonly use convex over-approximations of the activation functions in order to formulate a convex verification problem. As mentioned previously, we investigate the scalability of semidefinite programming methods [36] in this work. The authors in [37] present an early work in this direction, encoding ReLU activations via semidefinite constraints. This

was improved upon in DeepSDP [6], which can handle arbitrary activations — so long as they are encodable via quadratic constraints. The work of [7] recognized that certain restricted parameterizations of DeepSDP admit sparsity structures amenable to chordal decomposition, but such formulations tend to be conservative and also limiting in their expressiveness. The notion of chordal sparsity has proven useful in decomposing large-scale optimization problems, and are extensively studied [8], [9], [10], [38], [39] with application in [40], [41], [42]. Some recent directions on SDP-based neural network verification have examined finding tighter abstractions, especially for networks with ReLU activations [43], [44]. Also related are works based on polynomial optimization [45], [46], [47], [48], which similarly use semidefinite programming as the underlying computational technique.

II. BACKGROUND AND PROBLEM FORMULATION

We consider feedforward neural networks $f : \mathbb{R}^{n_1} \rightarrow \mathbb{R}^m$ with $K \geq 2$ layers, i.e., $K - 1$ hidden layers. For an input $x_1 \in \mathbb{R}^{n_1}$, the output of the neural network is recursively computed for $k = 1, \dots, K - 1$ as

$$f(x_1) := W_K x_K + b_K, \quad x_{k+1} := \phi(W_k x_k + b_k),$$

where W_k and b_k are the weight matrices and bias vectors of the k th layer that are of appropriate dimensions. We denote the dimensions of x_1, \dots, x_K by positive integers $n_1, \dots, n_K \in \mathbb{Z}_+$. The function $\phi(u) := \text{vcat}(\varphi(u_1), \varphi(u_2), \dots)$ is the vector-valued result of the activation function $\varphi : \mathbb{R} \rightarrow \mathbb{R}$ applied element-wise to the input $u = \text{vcat}(u_1, u_2, \dots)$. We assume throughout the paper that the same type of activation function is used for all neurons. Let $N := n_1 + \dots + n_K$ and also define the stacked vectors

$$\mathbf{x} := \text{vcat}(x_1, \dots, x_K) \in \mathbb{R}^N, \quad \mathbf{z} := \text{vcat}(\mathbf{x}, 1) \in \mathbb{R}^{N+1},$$

with selectors $E_a \mathbf{z} = 1$ and $E_k \mathbf{z} = x_k$ for $k = 1, \dots, K$.

A. Neural Network Verification with DeepSDP

Towards verifying if a network f satisfies a specification \mathcal{S} , the authors in [6] have presented DeepSDP. The main idea is to use *quadratic constraints* (QCs) to abstract the input set \mathcal{X} , the activation functions ϕ , and the safety specification \mathcal{S} . We then use these QCs to set up the safety verification problem as a large *semidefinite program* (SDP) whose satisfiability implies that the network is safe.

1) *Abstracting the Input Set via QCs*: To abstract the input set \mathcal{X} into a QC, let $P(\gamma_{\text{in}}) \in \mathbb{S}^{n_1+1}$ be a symmetric indefinite matrices parametrized by a vector $\gamma_{\text{in}} \in \Gamma_{\text{in}}$ where Γ_{in} is the permissible set. Each such matrix $P(\gamma_{\text{in}})$ now has to satisfy the following QC

$$\mathbf{z}^\top Z_{\text{in}} \mathbf{z} \geq 0, \quad Z_{\text{in}} := \begin{bmatrix} E_1 \\ E_a \end{bmatrix}^\top P(\gamma_{\text{in}}) \begin{bmatrix} E_1 \\ E_a \end{bmatrix} \in \mathbb{S}^{N+1} \quad (1)$$

where recall that $E_1 \mathbf{z} = x_1$ and $E_a \mathbf{z} = 1$. The vector γ_{in} appears linearly in $P(\gamma_{\text{in}})$ and will be a decision variable in DeepSDP. The dimension of γ_{in} depends on the specific

choice of $P(\gamma_{\text{in}})$ (see [6, Section 3.A]): for instance, the polytope $\mathcal{X} := \{x_1 \in \mathbb{R}^n : Hx \leq h\}$ can be abstracted into the QC (1) with

$$P(\gamma_{\text{in}}) := \begin{bmatrix} H^\top \Lambda H & -H^\top \Lambda h \\ -h^\top \Lambda H & h^\top \Lambda h \end{bmatrix}$$

where Λ is a symmetric and nonnegative matrix whose entries are those of γ_{in} . As the entries of Λ are nonnegative, in this case Γ_{in} is the set of nonnegative vectors.

2) *Abstracting the Activation Functions via QCs:* To abstract the activation function $\phi : \mathbb{R}^n \rightarrow \mathbb{R}^n$, let $Q(\gamma_{\text{ac}}) \in \mathbb{S}^{2n+1}$ be a set of symmetric indefinite matrices parametrized by a vector $\gamma_{\text{ac}} \in \Gamma_{\text{ac}}$ where Γ_{ac} is the permissible set. Each such matrix $Q(\gamma_{\text{ac}})$ must now satisfy the following QC

$$\begin{bmatrix} u \\ \phi(u) \\ 1 \end{bmatrix}^\top Q(\gamma_{\text{ac}}) \begin{bmatrix} u \\ \phi(u) \\ 1 \end{bmatrix} \geq 0 \text{ for all } u \in U \quad (2)$$

where $U \subseteq \mathbb{R}^n$ is some input set of ϕ . The dimension of γ_{ac} depends on the particular activation function and on the specific abstraction that is chosen. In particular, it was shown in [6, Proposition 2] that many activations φ are $[a, b]$ -sector-bounded¹ for fixed scalars $a \leq b$. In such cases, the stacked activation $\phi(u) = \text{vcat}(\varphi(u_1), \varphi(u_2), \dots)$ admits the abstraction

$$Q_{\text{sec}} := \begin{bmatrix} -2abT & (a+b)T & q_{13} \\ (a+b)T & -2T & q_{23} \\ q_{13}^\top & q_{23}^\top & q_{33} \end{bmatrix} \in \mathbb{S}^{1+2n}, \quad (3)$$

$$T := \sum_{i=1}^n \lambda_{ii} e_i e_i^\top + \sum_{(i,j) \in \mathcal{I}_\beta} \lambda_{ij} \Delta_{ij} \Delta_{ij}^\top,$$

$$\mathcal{I}_\beta := \{(i, j) : 1 \leq i < j \leq n, j - i \leq \beta\}$$

where $\Delta_{ij} = e_i - e_j$, and $q_{13}, q_{23}, q_{33}, \lambda_{ij}$ are linearly parametrized by γ_{ac} . Here \mathcal{I}_β is a β -banded index set, which means that T is a β -banded symmetric matrix. Importantly, this abstraction for activations can be done the entire multi-layered network and not just for a single layer's activation. By defining $b := \text{vcat}(b_1, \dots, b_{K-1})$,

$$A := \begin{bmatrix} W_1 & \cdots & 0 & 0 \\ \vdots & \ddots & \vdots & \vdots \\ 0 & \cdots & W_{K-1} & 0 \end{bmatrix}, \quad B := \begin{bmatrix} 0 & I_{n_2} & \cdots & 0 \\ \vdots & \vdots & \ddots & \vdots \\ 0 & 0 & \cdots & I_{n_K} \end{bmatrix},$$

we may write $Bx = \phi(Ax + b) \in \mathbb{R}^{n_2 + \dots + n_K}$, such that (2) then becomes

$$\mathbf{z}^\top Z_{\text{ac}} \mathbf{z} \geq 0, \quad Z_{\text{ac}} := \begin{bmatrix} \star \\ \star \end{bmatrix}^\top Q(\gamma_{\text{ac}}) \begin{bmatrix} A & b \\ B & 0 \\ 0 & 1 \end{bmatrix} \in \mathbb{S}^{N+1}, \quad (4)$$

where we use $[\star]$ to denote identical terms as on the RHS and we assume that $Q(\gamma_{\text{ac}}) = Q_{\text{sec}}$. The use of the integer-valued β parameter in T serves to induce sparsity² in Z_{ac} so

¹A function φ is $[a, b]$ -sector-bounded if $a \leq \frac{\varphi(u_1) - \varphi(u_2)}{u_1 - u_2} \leq b$ for all $u_1, u_2 \in \mathbb{R}$. For instance, the ReLU, sigmoid, and tanh activations are all $[0, 1]$ -sector bounded.

²In the original formulation of Q_{sec} in [6, Section 3.C] the authors do not assume a banded index set. This is equivalent to the case of taking $\beta = N - n_1 - 1$ under our formulation.

that we may apply chordal decomposition later. Intuitively, fixing larger values of β permits more λ_{ij} terms, thereby increasing slack (and thus accuracy) in the abstraction at the cost of sparsity (and thus scalability). Our formulation therefore allows one to use β as a tunable sparsity parameter to navigate this accuracy-scalability trade-off.

We remark that the DeepSDP framework is not restricted to abstractions of form Q_{sec} . However, we will first present our main results under the assumptions of (2) with $Q(\gamma_{\text{ac}}) = Q_{\text{sec}}$ in Section III before showing in Section IV how other abstractions may be incorporated while preserving sparsity.

3) *Abstracting the Safety Specification via QCs:* To abstract the safety specification \mathcal{S} into a QC, let $S \in \mathbb{S}^{n_1+m+1}$ be a symmetric matrix. We assume that S encodes safety by the inequality $\mathbf{z}^\top Z_{\text{out}} \mathbf{z} \geq 0$ where

$$Z_{\text{out}} := \begin{bmatrix} \star \\ \star \end{bmatrix}^\top S \begin{bmatrix} I & 0 & 0 \\ 0 & W_K & b_K \\ 0 & 0 & 1 \end{bmatrix} \begin{bmatrix} E_1 \\ E_K \\ E_a \end{bmatrix} \in \mathbb{S}^{N+1}, \quad (5)$$

which captures a quadratic relation between the input x_1 and output $y = f(x_1)$. For instance, to bound the local L_2 gain via $S = \{(x_1, y) : \|y\|^2 \leq \kappa \|x_1\|^2\}$, take $S = \text{diag}(-\kappa I, I, 0)$.

4) *DeepSDP:* Finally, we combine the input, activation, and output QCs and define DeepSDP as the following semidefinite program:

$$\begin{aligned} & \text{find } \gamma := (\gamma_{\text{in}}, \gamma_{\text{ac}}) \in \Gamma_{\text{in}} \times \Gamma_{\text{ac}} \\ & \text{subject to } Z(\gamma) := Z_{\text{in}} + Z_{\text{ac}} + Z_{\text{out}} \preceq 0, \end{aligned} \quad (6)$$

We recall the formal safety guarantees of DeepSDP next.

Lemma 1 ([6], Theorem 2). *Suppose DeepSDP (6) is feasible, then f satisfies the specification \mathcal{S} .*

This result ensures that feasibility of DeepSDP implies that the desired safety condition \mathcal{S} holds. Moreover, one can also derive a *reachability* variant of DeepSDP by parametrizing some components of S e.g. the L_2 gain κ in the above example, in order to then optimize for the tightest fit. This notion of reachability is demonstrated in [6, Section 5] and also in Section V. A computational bottleneck of DeepSDP, however, is the large semidefinite constraint. In particular, the dimension of $Z(\gamma)$ grows with the size of the neural network f , so that solving DeepSDP quickly becomes intractable.

B. Chordal Sparsity

The notion of chordal sparsity connects chordal graph theory and sparse matrix decomposition [49], [9], and can be used to efficiently solve large-scale semidefinite programs. In the context of this paper, if $Z(\gamma)$ is chordally sparse, then the LMI constraint $Z(\gamma) \preceq 0$ within DeepSDP can be split into an equivalent set of smaller matrix constraints.

1) *Chordal Graphs and Sparse Matrices:* Let $\mathcal{G}(\mathcal{V}, \mathcal{E})$ be a graph with vertices $\mathcal{V} = [n] := \{1, \dots, n\}$ and edges $\mathcal{E} \subseteq \mathcal{V} \times \mathcal{V}$. We assume that \mathcal{G} is undirected, meaning that \mathcal{E} is symmetric, i.e., $(i, j) \in \mathcal{E}$ implies $(j, i) \in \mathcal{E}$. A subset of vertices $\mathcal{C} \subseteq \mathcal{V}$ forms a *clique* if $u, v \in \mathcal{C}$ implies that $(u, v) \in \mathcal{E}$, and let $\mathcal{C}(i)$ be the i th vertex of \mathcal{C} under

the natural ordering. If there is no other clique that strictly contains \mathcal{C} , then \mathcal{C} is a *maximal clique*. A cycle of length k is a sequence of vertices $v_1, \dots, v_k, v_1 \in \mathcal{V}$ with $(v_k, v_1) \in \mathcal{E}$ and adjacent connections $(v_i, v_{i+1}) \in \mathcal{E}$. A *chord* is an edge that connects two nonadjacent vertices in a cycle. We say that a graph is *chordal* if every cycle of length ≥ 4 has at least one chord [9, Chapter 2].

Dually, an edge set \mathcal{E} may also describe the sparsity of a symmetric matrix. Given $\mathcal{G}(\mathcal{V}, \mathcal{E})$, the set of symmetric matrices of size n with sparsity pattern \mathcal{E} is defined as

$$\mathbb{S}^n(\mathcal{E}) := \{X \in \mathbb{S}^n : X_{ij} = X_{ji} = 0 \text{ if } (i, j) \notin \mathcal{E}\}. \quad (7)$$

If $X \in \mathbb{S}^n(\mathcal{E})$, then we say that X has sparsity pattern \mathcal{E} . We say that the entry X_{ij} is *sparse* if $(i, j) \notin \mathcal{E}$, and that it is *dense* otherwise. Moreover, if $\mathcal{G}(\mathcal{V}, \mathcal{E})$ is chordal, then we say that X has *chordal sparsity* or is *chordally sparse*.

2) *Chordal Decomposition of Sparse Matrices*: For a chordally sparse matrix $X \in \mathbb{S}^n(\mathcal{E})$, one can deduce whether $X \succeq 0$ by analyzing the maximal cliques of $\mathcal{G}(\mathcal{V}, \mathcal{E})$. To do this, given a clique $\mathcal{C} \subseteq \mathcal{V}$, define its projection matrix $E_{\mathcal{C}} \in \mathbb{R}^{|\mathcal{C}| \times n}$ such that $(E_{\mathcal{C}})_{ij} = 1$ iff $\mathcal{C}(i) = j$, and $(E_{\mathcal{C}})_{ij} = 0$ otherwise. An exact condition for $X \succeq 0$ is then stated as follows.

Lemma 2 ([10] Theorem 2.10). *Let $\mathcal{G}(\mathcal{V}, \mathcal{E})$ be a chordal and $\{\mathcal{C}_1, \dots, \mathcal{C}_p\}$ its maximal cliques. Then $X \in \mathbb{S}^n(\mathcal{E})$ and $X \succeq 0$ iff there are $X_k \in \mathbb{S}^{|\mathcal{C}_k|}$ such that each $X_k \succeq 0$ and $X = \sum_{k=1}^p E_{\mathcal{C}_k}^\top X_k E_{\mathcal{C}_k}$.*

We call this summation of X_k a *chordal decomposition* of X . The importance of this result is that we may now solve a large LMI using an equivalent collection of smaller ones. Because solving $X \succeq 0$ is typically at least n^3 in time [50], this trade-off for smaller $X_k \succeq 0$ is often desirable.

III. NEURAL NETWORK VERIFICATION WITH CHORDAL-DEEPSDP

In this section, we construct a chordally sparse variant of DeepSDP that we call Chordal-DeepSDP. We assume here that activation functions are abstracted as sector bounded functions with $Q(\gamma_{\text{ac}}) = Q_{\text{sec}}$, and show in Section IV how other abstractions can be used while preserving sparsity. The main technical challenge is to precisely characterize the sparsity of $Z(\gamma)$, and to gain intuition we show in Figure 1 different patterns as the value of β varies.

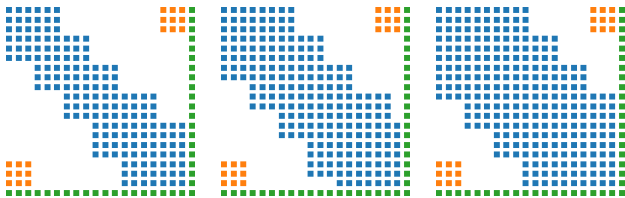


Fig. 1. The sparsity of $Z(\gamma) \in \mathbb{S}^{N+1}$ for $\beta = 0, 2, 4$ for networks with depth $K = 6$ and $n_k = 3$ for each k . Each plot corresponds to a sparsity \mathcal{E}_β where $(i, j) \in \mathcal{E}_\beta$ iff (i, j) is a colored square. Each \mathcal{E}_β is the disjoint union of: \mathcal{E}_M (blue), \mathcal{E}_a (green), and $\mathcal{E}_{1,K}$ (orange).

We see that \mathcal{E}_β is an overlapping block-diagonal matrix with arrow structure [9]. For each increment of β , we observe

that the blocks on the diagonal grow one unit downwards and rightwards. From these plots it is straightforward to conjecture the structure of \mathcal{E}_β . First, let us define the function $S(k) := n_1 + \dots + n_k$ to express summation over n_k , where $S(0) = 0$, $S(K) = N$, and let $n_{K+1} = m$. The sparsity patterns \mathcal{E}_β observed in Figure 1 are then characterized in the following lemma.

Lemma 3. *It holds that $Z(\gamma) \in \mathbb{S}^{N+1}(\mathcal{E}_\beta)$, where*

$$\mathcal{E}_\beta := \mathcal{E}_M \cup \mathcal{E}_a \cup \mathcal{E}_{1,K}$$

$$\mathcal{E}_M := \mathcal{E}_{M,1} \cup \dots \cup \mathcal{E}_{M,K-1},$$

$$\mathcal{E}_a := \{(i, j) \in [N+1]^2 : i = N+1 \text{ or } j = N+1\},$$

with each $\mathcal{E}_{M,k} \subseteq [N]^2$ and the $\mathcal{E}_{1,K} \subseteq [N]^2$ defined as

$$\mathcal{E}_{M,k} := \{(i, j) : S(k-1) + 1 \leq i, j \leq S(k+1) + \beta\},$$

$$\mathcal{E}_{1,K} := \{(i, j) : (1 \leq i \leq n_1 \text{ and } S(K-1) + 1 \leq j \leq N) \text{ or } (1 \leq j \leq n_1 \text{ and } S(K-1) + 1 \leq i \leq N)\}.$$

However, a chordal decomposition of $Z(\gamma)$ given \mathcal{E}_β is not obvious. This is because each $\mathcal{G}([N+1], \mathcal{E}_\beta)$ is not chordal: the “wing tips” at the lower-left and upper-right corners allows for a chord-less cycle of length ≥ 4 between vertices 1 and $N+1$, akin to the “wheel” shape seen in [9, Figure 3.1 (right)].

Crucially, however, the notion of chordal sparsity is tied to *graphs* rather than to *matrices*. For instance, given $Z(\gamma) \in \mathbb{S}^{N+1}(\mathcal{E}_\beta)$, if there exists $\mathcal{F}_\beta \supseteq \mathcal{E}_\beta$, then $Z(\gamma) \in \mathbb{S}^{N+1}(\mathcal{F}_\beta)$ as well. Moreover, if $\mathcal{G}([N+1], \mathcal{F}_\beta)$ is chordal, then one may decompose $Z(\gamma)$ with respect to the maximal cliques of $\mathcal{G}([N+1], \mathcal{F}_\beta)$ as in Lemma 2. Such \mathcal{F}_β is known as a *chordal extension* of \mathcal{E}_β , and the flexibility of permitting a matrix to have multiple valid sparsity patterns means that we may pick whichever sparsity is convenient (i.e. chordal) in order to apply chordal decomposition.

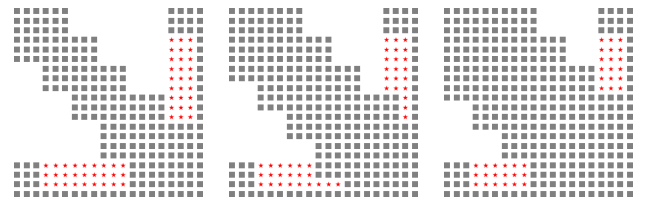


Fig. 2. A chordal extension of each \mathcal{E}_β into \mathcal{F}_β , such that each $\mathcal{G}([N+1], \mathcal{F}_\beta)$ is now chordal.

One such chordal extension of each \mathcal{E}_β is shown in Figure 2, where the idea is to fill in certain rows and columns (denoted by red \star) in order to chordally extend each \mathcal{E}_β into its corresponding \mathcal{F}_β . This chordal extension in Figure 2 can be described by $\mathcal{F}_\beta := \mathcal{E}_\beta \cup \mathcal{E}_K$, where $\mathcal{E}_K \subseteq [N+1]^2$ with

$$\mathcal{E}_K := \{(i, j) : S(K-1) + 1 \leq i \leq N$$

$$\text{or } S(K-1) + 1 \leq j \leq N\}.$$

The sparsity patterns \mathcal{F}_β are central to our sparsity analysis of $Z(\gamma)$ and chordal decomposition of DeepSDP. We next describe the chordality and maximal cliques of $\mathcal{G}([N+1], \mathcal{F}_\beta)$.

Theorem 1. *The graph $\mathcal{G}([N+1], \mathcal{F}_\beta)$ is chordal and the number of its maximal cliques is*

$$p := \min\{k : S(k+1) + \beta \geq S(K-1)\}.$$

Furthermore, the k th maximal clique for $k < p$ is

$$\mathcal{C}_k := \{v : S(k-1) + 1 \leq v \leq S(k+1) + \beta \\ \text{or } S(K-1) + 1 \leq v \leq N+1\},$$

and the final clique is $\mathcal{C}_p := \{v : S(p-1) + 1 \leq v \leq N+1\}$.

The above results establish that $Z(\gamma) \in \mathbb{S}^{N+1}(\mathcal{F}_\beta)$ and that $\mathcal{G}([N+1], \mathcal{F}_\beta)$ is chordal with maximal cliques $\{\mathcal{C}_1, \dots, \mathcal{C}_p\}$. These are the sufficient conditions for Lemma 2, allowing us to form a chordally sparse variant of DeepSDP below that we call Chordal-DeepSDP.

$$\begin{aligned} \text{find } \gamma := (\gamma_{\text{in}}, \gamma_{\text{ac}}) \in \Gamma_{\text{in}} \times \Gamma_{\text{ac}}, \\ Z_1, \dots, Z_p \preceq 0 \\ \text{subject to } Z(\gamma) = \sum_{k=1}^p E_{\mathcal{C}_k}^\top Z_k E_{\mathcal{C}_k} \end{aligned} \quad (8)$$

Moreover, by Lemma 2 we have that DeepSDP and Chordal-DeepSDP are in fact *equivalent problems*.

Theorem 2. *DeepSDP (6) and Chordal-DeepSDP (8) are equivalent: one is feasible iff the other is, and γ is a solution to (6) iff γ and some Z_1, \dots, Z_p is a solution to (8).*

Remark 1. *If Chordal-DeepSDP (8) is feasible, then the safety condition in Lemma 1 holds.*

In summary, we have decomposed the large semidefinite constraint $Z(\gamma) \preceq 0$ present in DeepSDP into a large equality constraint and a collection of smaller $Z_k \preceq 0$ constraints. The primary benefit of Chordal-DeepSDP is computational, since the cost of solving an LMI is usually at least cubic in its size [50]. This means that solving $Z(\gamma) \preceq 0$ is at least cubic in N , whereas the cost of each $Z_k \preceq 0$ is at least cubic in $|\mathcal{C}_k|$ — which may be significantly smaller than N . This is especially preferable for deeper networks, as the number of cliques grows with the number of layers.

Moreover, our formulation of Chordal-DeepSDP admits any symmetric S , meaning that this method can handle arbitrary quadratically-coupled input-output specifications. This is a key advantage over the more conservative approach of [7], which can only handle output constraints.

IV. BOLSTERING CHORDAL-DEEPSDP WITH DOUBLE DECOMPOSITION AND ADJACENT-LAYER ABSTRACTIONS

In Section III, we have built-up a basic version of Chordal-DeepSDP. In Section IV-A, we show that our formulation of \mathcal{F}_β from \mathcal{E}_β admits yet *another* level of chordal decomposition that we found useful for performance and that we call Chordal-DeepSDP-2. In addition, our construction until this point has only assumed $Q(\gamma) = Q_{\text{sec}}$ for abstracting activation functions ϕ . This simplifies the presentation of our theoretical results, as parametrization of Q_{sec} by different β is the primary difficulty in the sparsity analysis of $Z(\gamma)$. In practice, however, we found additional abstractions useful to

more tightly bound the activation behavior — in Section IV-B we show how to incorporate other activation abstractions that target adjacent-layer connections while preserving the same sparsity \mathcal{E}_β analyzed in Theorem 1.

A. Double Decomposition

In Section III, we presented a chordal decomposition of $Z(\gamma)$ with respect to the maximal cliques of $\mathcal{G}([N+1], \mathcal{F}_\beta)$. Recall, however, that we obtained \mathcal{F}_β from \mathcal{E}_β by treating certain zero entries of $Z(\gamma)$ as dense, see also Figure 2. This means that certain Z_k terms in the equality constraint of Chordal-DeepSDP will in fact have well-structured sparsity, which we state next.

Lemma 4. *Each matrix Z_k in Chordal-DeepSDP (8) for indices $2 \leq k \leq p-1$ has structure*

$$Z_k = \begin{bmatrix} (Z_k)_{11} & 0 & (Z_k)_{13} \\ 0 & (Z_k)_{22} & (Z_k)_{23} \\ (Z_k)_{13}^\top & (Z_k)_{23}^\top & (Z_k)_{33} \end{bmatrix},$$

where $(Z_k)_{11} \in \mathbb{S}^{n_k+n_{k+1}+\beta}$, $(Z_k)_{22} \in \mathbb{S}^{n_k}$, $(Z_k)_{33} \in \mathbb{R}$.

The structure of these Z_k in Lemma 4 is a block-arrow shape [9, Section 8.2], which are known to be chordal. In particular for $2 \leq k \leq p-1$ we may express a chordal decomposition of Z_k as

$$Z_k = E_{\mathcal{D}_{k,1}}^\top Y_{k,1} E_{\mathcal{D}_{k,1}} + E_{\mathcal{D}_{k,2}}^\top Y_{k,2} E_{\mathcal{D}_{k,2}} \in \mathbb{S}^{|\mathcal{C}_k|}(\mathcal{D}_{k,1} \cup \mathcal{D}_{k,2})$$

where the two maximal cliques for this block-arrow shape are $\mathcal{D}_{k,1}, \mathcal{D}_{k,2} \subseteq [|\mathcal{C}_k|]$ with

$$\begin{aligned} \mathcal{D}_{k,1} &:= \{v : 1 \leq v \leq n_k + n_{k+1} + \beta\} \cup \{|\mathcal{C}_k|\}, \\ \mathcal{D}_{k,2} &:= \{v : n_k + n_{k+1} + 1 \leq v \leq |\mathcal{C}_k|\}, \end{aligned}$$

where $\mathcal{D}_{k,1}$ covers the (11), (13), (33) blocks of Z_k , and $\mathcal{D}_{k,2}$ covers the (22), (23), (33) blocks. Applying Lemma 2 again means that $Z_k \preceq 0$ iff $Y_{k,1}, Y_{k,2} \preceq 0$. This additional level of decomposition on Z_k means that we may further chordally decompose Chordal-DeepSDP. For simplicity, when $k=1$ let us define $Y_{1,1} = Z_1$ with $\mathcal{D}_{1,1} = \mathcal{C}_1$, and $Y_{1,2} = 0$ with $\mathcal{D}_{1,2} = \emptyset$ (and similarly for $k=p$). This doubly decomposed problem, which we call Chordal-DeepSDP-2, is formulated as:

$$\begin{aligned} \text{find } \gamma := (\gamma_{\text{in}}, \gamma_{\text{ac}}) \in \Gamma_{\text{in}} \times \Gamma_{\text{ac}}, \\ Y_{1,1}, Y_{1,2}, \dots, Y_{p,1}, Y_{p,2} \preceq 0 \\ \text{subject to } Z(\gamma) = \sum_{k=1}^p E_{\mathcal{D}_{k,1}}^\top Y_{k,1} E_{\mathcal{D}_{k,1}} + E_{\mathcal{D}_{k,2}}^\top Y_{k,2} E_{\mathcal{D}_{k,2}} \end{aligned} \quad (9)$$

Remark 2. *DeepSDP (6), Chordal-DeepSDP (8), and Chordal-DeepSDP-2 (9) are equivalent problems in the sense of Theorem 2 due to Lemma 2.*

B. Adjacent-Layer Abstractions

Often it is desirable to use multiple activation abstractions in order to tightly bound the network behavior. More generally, we say that $Q_k \in \mathbb{S}^{1+2n_{k+1}}$ is an abstraction for

the adjacent-layer connection $x_{k+1} = \phi(W_k x_k + b_k)$ if the following inequality holds:

$$\begin{bmatrix} \star \\ \star \end{bmatrix}^\top Q_k \begin{bmatrix} W_k & 0 & b_k \\ 0 & I_{n_{k+1}} & 0 \\ 0 & 0 & 1 \end{bmatrix} \begin{bmatrix} E_k \\ E_{k+1} \\ E_a \end{bmatrix} \mathbf{z} \geq 0 \quad (10)$$

for all $x_k \in \mathcal{X}_k$, where \mathcal{X}_k includes the reachable set of x_k from $x_1 \in \mathcal{X}_1$. Such Q_k can encode useful information about the activations at each layer. For instance, if one knows from $x_1 \in \mathcal{X}$ that x_k always satisfies $\underline{x}_k \leq x_k \leq \bar{x}_k$, then Q_{k-1} can encode the fact that x_k lies within this box, similar to [6, Section 3.C.4]. Using interval bounds is popular in practice because they are typically cheap to compute, and we use the LiRPA library [51] for this, though other interval preprocessing choices are also valid.

Note that the nonnegativity in (10) means we may *add* abstractions to yield new ones. Thus, the inequality

$$\sum_{k=1}^{K-1} \begin{bmatrix} \star \\ \star \end{bmatrix}^\top Q_k \begin{bmatrix} W_k & 0 & b_k \\ 0 & I_{n_{k+1}} & 0 \\ 0 & 0 & 1 \end{bmatrix} \begin{bmatrix} E_k \\ E_{k+1} \\ E_a \end{bmatrix} \mathbf{z} \geq 0 \quad (11)$$

for all $x_1 \in \mathcal{X}$, would be an abstraction that accounts for *all* $K-1$ adjacent-layer connections in the network. Importantly, the formulation of (11) permits us to use a combination of *arbitrary* abstractions Q_k for ϕ between adjacent layers, so long as they each satisfy the appropriate QC. In addition, we may also rewrite (11) into a form resembling that of (4), which we show in Lemma 5

Lemma 5. *There exists Q_{adj} linearly parametrized by the Q_1, \dots, Q_{K-1} such that the inequality*

$$\mathbf{z}^\top \begin{bmatrix} A & b \\ B & 0 \\ 0 & 1 \end{bmatrix}^\top Q_{\text{adj}} \begin{bmatrix} A & b \\ B & 0 \\ 0 & 1 \end{bmatrix} \mathbf{z} \geq 0 \text{ for all } x_1 \in \mathcal{X}$$

holds iff the inequality (11) holds.

Applying again the nonnegativity condition of activation QCs, we can redefine $Q(\gamma_{\text{ac}}) := Q_{\text{sec}} + Q_{\text{adj}}$. Intuitively Q_{sec} is able to enforce *cross-layer* dependencies, while Q_{adj} can only enforce adjacent-layer dependencies. Although different abstractions come with their respective trade-offs, combining them into a single $Q(\gamma_{\text{ac}})$ for DeepSDP means that we can more tightly approximate the activation functions of the entire multi-layered network. Conveniently, using such a Q_{adj} does not change the overall sparsity of $Z(\gamma)$ as we will show next.

Theorem 3. *Let $Q(\gamma_{\text{ac}}) := Q_{\text{sec}} + Q_{\text{adj}}$ and similarly define $Z(\gamma)$ as before, then $Z(\gamma) \in \mathbb{S}^{N+1}(\mathcal{E}_\beta)$.*

This means that the formulations of Chordal-DeepSDP and Chordal-DeepSDP-2 are still equivalent to DeepSDP under the definition of $Q(\gamma_{\text{ac}})$ in Theorem 3.

V. NUMERICAL EXPERIMENTS

We now evaluate the effectiveness of our approach, where we aim to answer the following: **(Q1)** What is the scalability of our methods vs DeepSDP? **(Q2)** What is the impact

of β on verification accuracy? We refer to [6] for other experiments on the accuracy of DeepSDP, and recall that given a fixed β , the formulations of DeepSDP, Chordal-DeepSDP, and Chordal-DeepSDP-2 are equivalent.

a) QC Configuration: For ReLU functions, we use the sector-bounded QC proposed in [6, Lemma 4] and for general sector-bounded activations we use that of [6, Lemma 2]. Both of these have the same sparsity as Q_{sec} described in (3). We use Q_{adj} to encode interval propagation information that we obtain from the LiRPA library [51], similar to the *bounded nonlinearities* presented in [6, Section 3.C.4]. All of these activation QCs induce a $Z(\gamma)$ with sparsity \mathcal{E}_β .

b) Dataset: As our primary focus is on improving the scalability of DeepSDP under parametrized sparsity, we use two randomly generated datasets in our experiments: one batch for *scalability* experiments, and another batch for *reachability* experiments. We generate a collection of networks of widths = 10, 20 and depths $(K-1) = 5, 10, \dots, 50$ with Gaussian random weights with $\sigma := 2/\sqrt{w \log w}$ for scalability experiments and $\sigma := 1/\sqrt{2}$ for reachability experiments. We consider only ReLU activations. For ease of plotting, each of these networks have input and output dimensions $n_1 := m := 2$.

c) System: All experiments were run on machines with Intel Xeon Gold 6148 CPU @ 2.40 GHz with 80 cores and 692 GB of RAM. Our codebase was implemented with Julia 1.7.2 and we used MOSEK 9.3 as our convex solver.

A. (Q1): Scalability

For each random network we ran DeepSDP, Chordal-DeepSDP, and Chordal-DeepSDP-2 with $\beta = 0, \dots, 7$ to optimize a reachability ellipsoid when the initial input is constrained to the box $\mathcal{X} := \{x : \|\mathbf{1} - x\|_\infty \leq 0.5\} \subseteq \mathbb{R}^2$, where $\mathbf{1} \in \mathbb{R}^2$ is the vector of ones.

Our plots are shown in Figure 3. We observe that Chordal-DeepSDP-2 consistently outperforms both DeepSDP and Chordal-DeepSDP, especially as the network depth increases. While DeepSDP with $\beta = 0$ is competitive, its performance quickly degrades as one increases β — whereas the decay for Chordal-DeepSDP and Chordal-DeepSDP-2 is more gradual, meaning that we can achieve more accuracy without a significant performance penalty.

B. (Q2): Reachability

We next investigate the impact of β on the verification accuracy. We first fix an initial set to be the box $\mathcal{X} := \{x : \|\mathbf{1} - x\|_\infty \leq 0.5\} \subseteq \mathbb{R}^2$, where $\mathbf{1} \in \mathbb{R}^2$ is the vector of ones. Then, we uniformly sample 10^5 points to approximate the center $y_c \in \mathbb{R}^2$ and shape $P \in \mathbb{S}_+^2$ — which is a regularized positive definite covariance matrix. The reachability problem is to then minimize ρ subject to $\|P^{-1}(y - y_c)\|^2 \leq \rho$, for which S takes form described in [6, Section 5.A]. Note that we fix P and y_c in contrast to the technique presented in [52], which allows for one to optimize over P and y_c directly at the cost of a larger semidefinite program.

We show the reach ellipsoids in Figure 4 along with uniformly sampled outputs. As the value of β increases, we see that the reach-set estimation becomes more accurate.

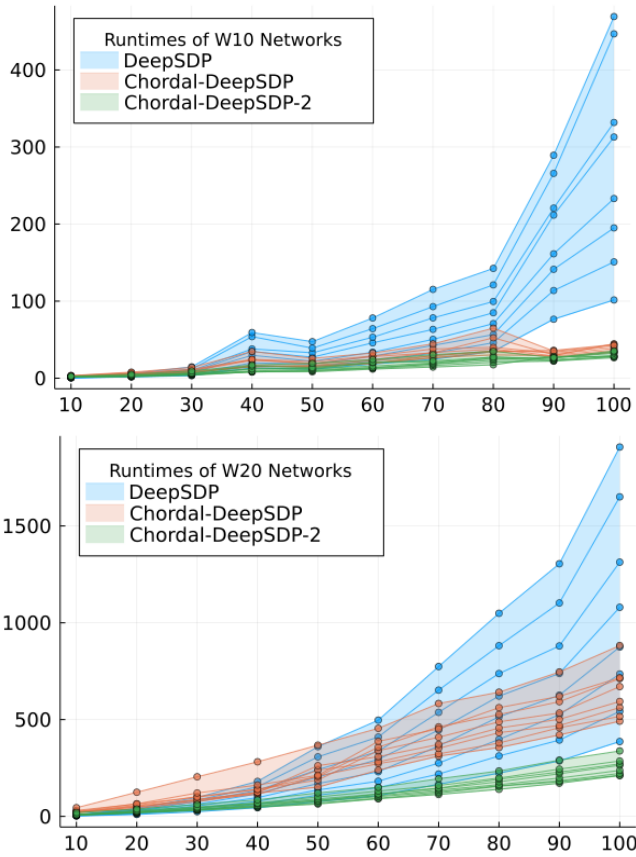


Fig. 3. Runtimes (secs) for DeepSDP (dualized), Chordal-LipSDP, and Chordal-LipSDP-2 on networks with widths 10, 20 and depths 10, 20, ..., 100. Each curve of the same color denote the performance of a different $\beta = 0, 1, \dots, 7$, with the intermediate region shaded. We observed that dualizing DeepSDP yields a significant performance increase compared to the primal (often over $\times 10$), but this benefit was not observed for Chordal-DeepSDP nor Chordal-DeepSDP-2.

C. Discussion

Our numerical experiments show that Chordal-DeepSDP-2 outperforms both DeepSDP and Chordal-DeepSDP on deep networks. Moreover, both Chordal-DeepSDP and Chordal-DeepSDP-2 exhibit better scaling properties than DeepSDP as the value of β increases, with the performance of DeepSDP significantly degrading.

We found it helpful to run the dual formulation of DeepSDP, with help of the `Dualization.jl` library³ — this alone achieves a very significant speedup (often over $\times 10$) compared to its primal formulation. This same dualization trick does not seem to benefit Chordal-DeepSDP nor Chordal-DeepSDP-2, however, likely because of the large equality constraint that is not present in DeepSDP.

VI. CONCLUSIONS

We present Chordal-DeepSDP, a SDP-based method for the safety verification of feedforward neural networks. Using

³As of this writing, `Dualization.jl` does not yet support dualizing a feasibility primal problem. We therefore add the simple objective of minimizing $\|\gamma\|_1$ for feasibility problems.

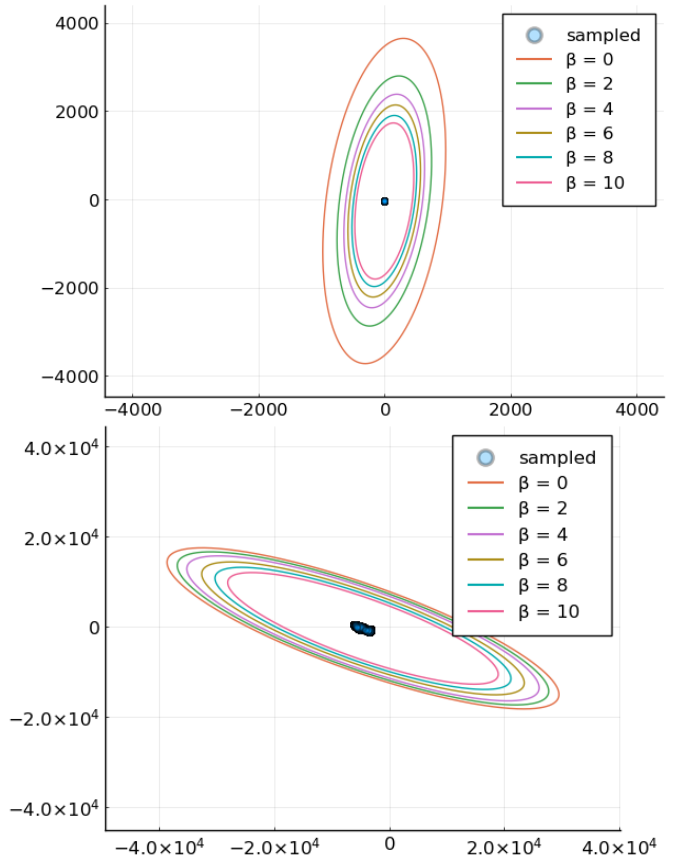


Fig. 4. Ellipsoid reachability for W10-D10 (top) and W20-D10 (bottom). As β increases, the ellipsoid tightens about the sampled points.

the concept of chordal sparsity, Chordal-DeepSDP presents a scalable chordal decomposition of DeepSDP. We show how to parametrically tune the sparsity of Chordal-SDP, allowing us to operate between the extremes of efficiency and accuracy. We provide numerical evaluations showcasing this trade-off in efficiency and accuracy and illustrate the computational advantages of Chordal-DeepSDP over DeepSDP.

APPENDIX

A. Results for Lemma 3

Proof of Lemma 3. By the Lemmas below, we have that

$$Z_{\text{in}} \in \mathbb{S}^{N+1}(\mathcal{E}_M \cup \mathcal{E}_a), \quad (\text{Lemma 6})$$

$$Z_{\text{ac}} \in \mathbb{S}^{N+1}(\mathcal{E}_M \cup \mathcal{E}_a), \quad (\text{Lemma 7})$$

$$Z_{\text{out}} \in \mathbb{S}^{N+1}(\mathcal{E}_M \cup \mathcal{E}_a \cup \mathcal{E}_{1,K}), \quad (\text{Lemma 8})$$

and so the sum $Z_{\text{in}} + Z_{\text{ac}} + Z_{\text{out}} = Z(\gamma) \in \mathbb{S}^{N+1}(\mathcal{E}_\beta)$. \square

Remark 3. Suppose that a graph has $n = 4$ vertices and $\mathcal{C} = \{1, 2, 4\}$, then the projection matrix $E_{\mathcal{C}}$ has the useful algebraic property for any $X \in \mathbb{S}^3$:

$$E_{\mathcal{C}}^{\top} X E_{\mathcal{C}} = \begin{bmatrix} X_{11} & X_{12} & 0 & X_{14} \\ X_{21} & X_{22} & 0 & X_{24} \\ 0 & 0 & 0 & 0 \\ X_{41} & X_{42} & 0 & X_{44} \end{bmatrix}.$$

This is convenient for quickly determining which entries of $Z_{\text{in}}, Z_{\text{ac}}, Z_{\text{out}}$ are dense.

Lemma 6. *It holds that $Z_{\text{in}} \in \mathbb{S}^{N+1}(\mathcal{E}_M \cup \mathcal{E}_a)$.*

Proof. Recall (1) and observe that $(Z_{\text{in}})_{ij}$ is dense iff

$$i, j \in \underbrace{\{v : 1 \leq v \leq n_1\}}_{\mathcal{B}_1} \cup \underbrace{\{v : v = N + 1\}}_{\mathcal{B}_a}$$

where $\mathcal{B}_1, \mathcal{B}_a \subseteq [N + 1]$ are disjoint. Equivalently, $(Z_{\text{in}})_{ij}$ is dense iff any of the following conditions hold:

- (1) $i \in \mathcal{B}_1$ and $j \in \mathcal{B}_1$
- (2) $i \in \mathcal{B}_1$ and $j \in \mathcal{B}_a$ (or the symmetric case)
- (3) $i \in \mathcal{B}_a$ and $j \in \mathcal{B}_a$

If (1) holds, then $(i, j) \in \mathcal{E}_{M,1}$; if any of (2) or (3) holds, then $(i, j) \in \mathcal{E}_a$. Thus (i, j) dense implies $(i, j) \in \mathcal{E}_M \cup \mathcal{E}_a$, and so $Z_{\text{in}} \in \mathbb{S}^{N+1}(\mathcal{E}_M \cup \mathcal{E}_a)$. \square

Lemma 7. *It holds that $Z_{\text{ac}} \in \mathbb{S}^{N+1}(\mathcal{E}_M \cup \mathcal{E}_a)$.*

Proof. Recall (4) and observe that we may express Z_{ac} as:

$$\begin{aligned} Z_{\text{ac}} &= \begin{bmatrix} A & b \\ B & 0 \\ 0 & 1 \end{bmatrix}^\top \begin{bmatrix} a_{11}T & a_{12}T & q_{13} \\ a_{12}T & a_{22}T & q_{23} \\ \star & \star & q_{33} \end{bmatrix} \begin{bmatrix} A & b \\ B & 0 \\ 0 & 1 \end{bmatrix} \\ &= \begin{bmatrix} \begin{bmatrix} A \\ B \end{bmatrix}^\top \begin{bmatrix} a_{11}T & a_{12}T \\ a_{12}T & a_{22}T \end{bmatrix} \begin{bmatrix} A \\ B \end{bmatrix} & \star \\ \star & \star \end{bmatrix} \\ &= \begin{bmatrix} M & p_{12} \\ \star & p_{22} \end{bmatrix} \in \mathbb{S}^{N+1} \end{aligned}$$

where $a_{11} := -2ab$, $a_{12} := a + b$, $a_{22} := -2$ and where p_{12} and p_{13} follow by straightforward calculation. From Lemma 9 (which is provided below) we know that $M \in \mathbb{S}^N(\mathcal{E}_M)$, and since p_{12}, p_{22} occupy the $(N + 1)$ th column and row of Z_{ac} , it follows that $Z_{\text{ac}} \in \mathbb{S}^{N+1}(\mathcal{E}_M \cup \mathcal{E}_a)$. \square

Lemma 8. *It holds that $Z_{\text{out}} \in \mathbb{S}^{N+1}(\mathcal{E}_M \cup \mathcal{E}_a \cup \mathcal{E}_{1,K})$.*

Proof. Recall (5) and observe that $(Z_{\text{out}})_{ij}$ is dense iff

$$\begin{aligned} i, j \in & \underbrace{\{v : 1 \leq v \leq n_1\}}_{\mathcal{B}_1} \\ & \cup \underbrace{\{v : S(K-1) + 1 \leq v \leq N\}}_{\mathcal{B}_K} \\ & \cup \underbrace{\{v : v = N + 1\}}_{\mathcal{B}_a}, \end{aligned}$$

where $\mathcal{B}_1, \mathcal{B}_K, \mathcal{B}_a \subseteq [N + 1]$ are disjoint. Equivalently, $(Z_{\text{out}})_{ij}$ is dense iff any of the following holds:

- (1) $i \in \mathcal{B}_1$ and $j \in \mathcal{B}_1$
- (2) $i \in \mathcal{B}_1$ and $j \in \mathcal{B}_K$ (or the symmetric case)
- (3) $i \in \mathcal{B}_1$ and $j \in \mathcal{B}_a$ (or the symmetric case)
- (4) $i \in \mathcal{B}_K$ and $j \in \mathcal{B}_K$
- (5) $i \in \mathcal{B}_K$ and $j \in \mathcal{B}_a$ (or the symmetric case)
- (6) $i \in \mathcal{B}_a$ and $j \in \mathcal{B}_a$

If (1) holds, then $(i, j) \in \mathcal{E}_{M,1}$; if (4) holds, then $(i, j) \in \mathcal{E}_{M,K-1}$; if (2) holds, then $(i, j) \in \mathcal{E}_{1,K}$; if any of (3), (5), or

(6) holds, then $(i, j) \in \mathcal{E}_a$. Thus (i, j) dense implies $(i, j) \in \mathcal{E}_M \cup \mathcal{E}_a \cup \mathcal{E}_{1,K}$, and so $Z_{\text{out}} \in \mathbb{S}^{N+1}(\mathcal{E}_M \cup \mathcal{E}_a \cup \mathcal{E}_{1,K})$. \square

Lemma 9. *For all $a_{11}, a_{12}, a_{22} \in \mathbb{R}$ it holds that*

$$M := \begin{bmatrix} A \\ B \end{bmatrix}^\top \begin{bmatrix} a_{11}T & a_{12}T \\ a_{12}T & a_{22}T \end{bmatrix} \begin{bmatrix} A \\ B \end{bmatrix} \in \mathbb{S}^N(\mathcal{E}_M).$$

Proof. This follows from [53, Theorem 1], in which the summation $S(k)$ is defined in the same manner, and in which the Z_α matrix from [53, Equation 3] has the same sparsity pattern as M . \square

B. Results for Theorem 1

Proof of Theorem 1. The definition of p lets us partition $\mathcal{F}_\beta = \mathcal{E}_A \cup \mathcal{E}_R$ with $\mathcal{E}_A \cap \mathcal{E}_R = \emptyset$, such that

$$\begin{aligned} \mathcal{E}_A &:= \mathcal{E}_{A,1} \cup \dots \cup \mathcal{E}_{A,p}, & \mathcal{E}_{A,k} &:= \mathcal{E}_{M,k} \cap [S(K-1)]^2 \\ \mathcal{E}_R &:= \{(i, j) : S(K-1) + 1 \leq i \text{ or } S(K-1) + 1 \leq j\}. \end{aligned}$$

with $\mathcal{E}_R \subseteq [N + 1]^2$. In other words, $\mathcal{E}_R = \mathcal{E}_K \cup \mathcal{E}_a$ and $\mathcal{E}_A = \mathcal{F}_\beta \setminus \mathcal{E}_R$. Our strategy is to show that $\mathcal{G}([S(K-1)], \mathcal{E}_A)$ is chordal and iteratively reconstruct $\mathcal{G}([N + 1], \mathcal{F}_\beta)$ using the edge set \mathcal{E}_R while preserving chordal sparsity at every step. To begin, we claim that the $\mathcal{G}([S(K-1)], \mathcal{E}_A)$ is chordal with maximal cliques $\mathcal{A}_1, \dots, \mathcal{A}_p$ where

$$\mathcal{A}_k = \{v \in [S(K-1)] : S(k-1) + 1 \leq v \leq S(k+1) + \beta\}.$$

This claim follows from [53, Theorem 2] if we identify the variable and notational substitutions

$$[S(K-1)] \mapsto \mathcal{V}, \quad S(K-1) \mapsto N, \quad \mathcal{E}_{A,k} \mapsto \mathcal{E}_k, \quad \beta \mapsto \tau.$$

Intuitively, \mathcal{E}_A is the same sparsity as in [53, Theorem 2] if one applies these mappings.

We now construct $\mathcal{G}([N + 1], \mathcal{F}_\beta)$ from $\mathcal{G}([S(K-1)], \mathcal{E}_A)$ by iteratively adding each vertex $v \in [N + 1] \setminus [S(K-1)]$ and its corresponding edges of \mathcal{E}_R . By the definition of \mathcal{E}_R , this iterative method means that each newly added v will have an edge to all the vertices already present. Inductively by Lemma 10 (which is provided below), this implies that $\mathcal{G}([N + 1], \mathcal{F}_\beta)$ is chordal and that its maximal cliques are

$$\mathcal{C}_k = \mathcal{A}_k \cup \{S(K-1) + 1, \dots, N + 1\}.$$

\square

Lemma 10. *Let $\mathcal{G}(\mathcal{V}, \mathcal{E})$ be a chordal graph and $\mathcal{C}_1, \dots, \mathcal{C}_p$ its maximal cliques, and let $\mathcal{G}'(\mathcal{V}', \mathcal{E}')$ be an extension of \mathcal{G} with a new vertex v' that is connected to every other vertex, i.e. $\mathcal{V}' = \mathcal{V} \cup \{v'\}$ and $\mathcal{E}' = \mathcal{E} \cup \{(v', v) : v \in \mathcal{V}\}$. Then \mathcal{G}' is chordal and its maximal cliques are $\mathcal{C}'_1, \dots, \mathcal{C}'_p$ where each $\mathcal{C}'_k = \mathcal{C}_k \cup \{v'\}$.*

Proof. Let u_1, \dots, u_k, u_1 be a cycle in \mathcal{G}' with $k \geq 4$. If this cycle lies strictly in \mathcal{G} , then there exists a chord because \mathcal{G} is chordal. Now suppose that $u_1 = v'$ without loss of generality, then the edge $(u_i, v') \in \mathcal{E}'$ for all vertices of this cycle by construction of \mathcal{G}' — meaning that there exists a chord. This shows that every cycle in \mathcal{G}' of length $k \geq 4$ has a chord, and thus \mathcal{G}' is chordal.

To show that each \mathcal{C}'_k is a maximal clique of \mathcal{G}' , suppose by contradiction that some \mathcal{C}'_k is strictly contained in another

clique \mathcal{C}' of \mathcal{G}' . But this means that $\mathcal{C}' \setminus \{v'\}$ is a clique in \mathcal{G} which strictly contains some $\mathcal{C}_k = \mathcal{C}'_k \setminus \{v'\}$, which contradicts the maximality assumption of each \mathcal{C}_k in \mathcal{G} .

To show that the \mathcal{C}'_k are the only maximal cliques of \mathcal{G}' , suppose by contradiction that there exists another maximal clique \mathcal{C}' of \mathcal{G}' . Now observe that $\mathcal{C}' \setminus \{v'\}$ is a clique in \mathcal{G} , and so by assumption it must be contained in some \mathcal{C}_k . However, this would mean that $\mathcal{C}' \subseteq \mathcal{C}'_k$, which contradicts the assumption that \mathcal{C}' is maximal in \mathcal{G}' . \square

C. Results for Theorem 2

Proof of Theorem 2. Since $Z(\gamma) \in \mathbb{S}^{N+1}(\mathcal{F}_\beta)$ and $\mathcal{G}([N+1], \mathcal{F}_\beta)$ is chordal with maximal cliques $\{\mathcal{C}_1, \dots, \mathcal{C}_p\}$, by Lemma 2 we have that $Z(\gamma) \preceq 0$ iff each $Z_k \preceq 0$ and $Z(\gamma) = \sum_{k=1}^p E_{\mathcal{C}_k}^\top Z_k E_{\mathcal{C}_k}$. \square

D. Results for Double Decomposition

Proof of Lemma 4. First, recall that $Z_{1 < k < p}$ has dimension $n_k + n_{k+1} + \beta + n_K + 1$ because:

$$\begin{aligned} \mathcal{C}_k &= \underbrace{\{v : S(k-1) + 1 \leq v \leq S(k+1) + \beta\}}_{n_k + n_{k+1} + \beta \text{ elements}} \\ &\cup \underbrace{\{v : S(K-1) + 1 \leq v \leq N + 1\}}_{n_K + 1 \text{ elements}}. \end{aligned}$$

To see why $(Z_k)_{12} = 0$, we show that its entries do not contribute any terms to $Z(\gamma)$. Let X_k be a dense matrix the same dimension as $(Z_k)_{12}$ and consider the expression:

$$E_{\mathcal{C}_k}^\top \begin{bmatrix} 0_{m_k \times m_k} & X_k & 0 \\ X_k^\top & 0_{n_K \times n_K} & 0 \\ 0 & 0 & 0_{1 \times 1} \end{bmatrix} E_{\mathcal{C}_k} \in \mathbb{S}^{N+1},$$

where $m_k = n_k + n_{k+1} + \beta$, whose (i, j) entry is dense iff

$$\begin{aligned} &(S(k-1) + 1 \leq i \leq S(k+1) + \beta \text{ and } S(K-1) + 1 \leq j \leq N) \\ &\text{or} \\ &(S(k-1) + 1 \leq j \leq S(k+1) + \beta \text{ and } S(K-1) + 1 \leq i \leq N). \end{aligned}$$

It will then suffice to show that $(i, j) \notin \mathcal{E}_\beta$ — which by Lemma 3 is a sparsity of $Z(\gamma)$ — because this allows us to conclude that $Z(\gamma)$ does not depend on $(Z_k)_{12}$. As this disjunctive condition is symmetric, we may consider some (i, j) satisfying the first case without loss of generality. First, $(i, j) \notin \mathcal{E}_M$ because our choice of $k < p$ means that

$$S(k-1) + 1 \leq i \leq S(k+1) + \beta < S(K-1) + 1 \leq j,$$

and so (i, j) does not meet the inclusion criteria of any $\mathcal{E}_{M,k}$. Furthermore, our choice of $k < p$ means that we cannot have $i = N + 1$ nor $j = N + 1$, and so $(i, j) \notin \mathcal{E}_a$. Finally, since $k > 1$, we have that $i, j \geq n_1 + 1$, and so $(i, j) \notin \mathcal{E}_{1,K}$. Consequently, it follows that $(Z_k)_{12} = 0$. \square

E. Results for Adjacent-Layer Connections

Proof of Lemma 5. We proceed by rewriting (11) into the form of Lemma 5.

$$\begin{aligned} &\sum_{k=1}^{K-1} \begin{bmatrix} \star \\ \star \end{bmatrix}^\top Q_k \begin{bmatrix} W_k & 0 & b_k \\ 0 & I_{n_{k+1}} & 0 \\ 0 & 0 & 1 \end{bmatrix} \begin{bmatrix} E_k \\ E_{k+1} \\ E_a \end{bmatrix} \mathbf{z} \\ &= \sum_{k=1}^{K-1} \begin{bmatrix} \star \\ \star \end{bmatrix}^\top Q_k \begin{bmatrix} W_k x_k + b_k \\ x_{k+1} \\ 1 \end{bmatrix} \\ &= \sum_{k=1}^{K-1} \begin{bmatrix} \star \\ \star \end{bmatrix}^\top P_k^\top Q_k P_k \begin{bmatrix} W_1 x_1 + b_1 \\ \vdots \\ W_{K-1} x_{K-1} + b_{K-1} \\ x_2 \\ \vdots \\ x_K \\ 1 \end{bmatrix} \\ &= \sum_{k=1}^{K-1} \begin{bmatrix} \star \\ \star \end{bmatrix}^\top P_k^\top Q_k P_k \begin{bmatrix} A & b \\ B & 0 \\ 0 & 1 \end{bmatrix} \mathbf{z} \\ &= \mathbf{z}^\top \begin{bmatrix} A & b \\ B & 0 \\ 0 & 1 \end{bmatrix}^\top \underbrace{\left(\sum_{k=1}^{K-1} P_k^\top Q_k P_k \right)}_{Q_{\text{adj}}} \begin{bmatrix} A & b \\ B & 0 \\ 0 & 1 \end{bmatrix} \mathbf{z} \end{aligned}$$

where P_k is a projection matrix acting on $\text{vcat}(A\mathbf{x}+b, B\mathbf{z}, \mathbf{1})$ that selects out the vector $\text{vcat}(W_k x_k + b_k, x_{k+1}, 1)$. \square

Proof of Theorem 3. It suffices to show that each summation term of (11) has sparsity \mathcal{E}_β . Consider the expression

$$\begin{bmatrix} \star \\ \star \end{bmatrix}^\top Q_k \begin{bmatrix} W_k & 0 & b_k \\ 0 & I_{n_{k+1}} & 0 \\ 0 & 0 & 1 \end{bmatrix} \begin{bmatrix} E_k \\ E_{k+1} \\ E_a \end{bmatrix},$$

whose (i, j) entry is dense iff

$$\begin{aligned} &i, j \in \underbrace{\{v : S(k-1) + 1 \leq v \leq S(k)\}}_{\mathcal{B}_k} \\ &\cup \underbrace{\{v : S(k) + 1 \leq v \leq S(k+1)\}}_{\mathcal{B}_{k+1}} \\ &\cup \underbrace{\{v : v = N + 1\}}_{\mathcal{B}_a}, \end{aligned}$$

where $\mathcal{B}_k, \mathcal{B}_{k+1}, \mathcal{B}_a$ are disjoint. Equivalently, the (i, j) entry is dense iff any of the following conditions holds:

- (1) $i \in \mathcal{B}_k$ and $j \in \mathcal{B}_k$
- (2) $i \in \mathcal{B}_k$ and $j \in \mathcal{B}_{k+1}$ (or the symmetric case)
- (3) $i \in \mathcal{B}_k$ and $j \in \mathcal{B}_a$ (or the symmetric case)
- (4) $i \in \mathcal{B}_{k+1}$ and $j \in \mathcal{B}_{k+1}$
- (5) $i \in \mathcal{B}_{k+1}$ and $j \in \mathcal{B}_a$ (or the symmetric case)
- (6) $i \in \mathcal{B}_a$ and $j \in \mathcal{B}_a$

If (1), (2), or (4) holds, then $(i, j) \in \mathcal{E}_{M,k}$; if (3), (5), or (6) holds, then $(i, j) \in \mathcal{E}_a$. Thus the (i, j) entry is dense implies that $(i, j) \in \mathcal{E}_M \cup \mathcal{E}_a$, and so $(i, j) \in \mathcal{E}_\beta$. \square

REFERENCES

- [1] D. Silver, T. Hubert, J. Schrittwieser, I. Antonoglou, M. Lai, A. Guez, M. Lanctot, L. Sifre, D. Kumaran, T. Graepel *et al.*, “A general reinforcement learning algorithm that masters chess, shogi, and go through self-play,” *Science*, vol. 362, no. 6419, pp. 1140–1144, 2018.
- [2] Y. LeCun, L. Bottou, Y. Bengio, and P. Haffner, “Gradient-based learning applied to document recognition,” *Proceedings of the IEEE*, vol. 86, no. 11, pp. 2278–2324, 1998.
- [3] A. Dosovitskiy, G. Ros, F. Codevilla, A. Lopez, and V. Koltun, “Carla: An open urban driving simulator,” in *Conference on robot learning*. PMLR, 2017, pp. 1–16.
- [4] I. J. Goodfellow, J. Shlens, and C. Szegedy, “Explaining and harnessing adversarial examples,” *arXiv preprint arXiv:1412.6572*, 2014.
- [5] J. Su, D. V. Vargas, and K. Sakurai, “One pixel attack for fooling deep neural networks,” *IEEE Transactions on Evolutionary Computation*, vol. 23, no. 5, pp. 828–841, 2019.
- [6] M. Fazlyab, M. Morari, and G. J. Pappas, “Safety verification and robustness analysis of neural networks via quadratic constraints and semidefinite programming,” *IEEE Transactions on Automatic Control*, 2020.
- [7] M. Newton and A. Papachristodoulou, “Exploiting sparsity for neural network verification,” in *Learning for Dynamics and Control*. PMLR, 2021, pp. 715–727.
- [8] J. Agler, W. Helton, S. McCullough, and L. Rodman, “Positive semidefinite matrices with a given sparsity pattern,” *Linear algebra and its applications*, vol. 107, pp. 101–149, 1988.
- [9] L. Vandenberghe and M. S. Andersen, “Chordal graphs and semidefinite optimization,” *Foundations and Trends in Optimization*, vol. 1, no. 4, pp. 241–433, 2015.
- [10] Y. Zheng, “Chordal sparsity in control and optimization of large-scale systems,” Ph.D. dissertation, University of Oxford, 2019.
- [11] S. Bak, C. Liu, and T. Johnson, “The second international verification of neural networks competition (vnn-comp 2021): Summary and results,” *arXiv preprint arXiv:2109.00498*, 2021.
- [12] C. Liu, T. Arnon, C. Lazarus, C. Strong, C. Barrett, and M. J. Kochenderfer, “Algorithms for verifying deep neural networks,” *arXiv preprint arXiv:1903.06758*, 2019.
- [13] G. Katz, C. Barrett, D. L. Dill, K. Julian, and M. J. Kochenderfer, “Reflux: An efficient smt solver for verifying deep neural networks,” in *International Conference on Computer Aided Verification*. Springer, 2017, pp. 97–117.
- [14] G. Katz, D. A. Huang, D. Ibeling, K. Julian, C. Lazarus, R. Lim, P. Shah, S. Thakoor, H. Wu, A. Zeljić *et al.*, “The marabou framework for verification and analysis of deep neural networks,” in *International Conference on Computer Aided Verification*. Springer, 2019, pp. 443–452.
- [15] X. Song, E. Manino, L. Sena, E. Alves, I. Bessa, M. Lujan, L. Cordeiro *et al.*, “Qnnverifier: A tool for verifying neural networks using smt-based model checking,” *arXiv preprint arXiv:2111.13110*, 2021.
- [16] L. Sena, X. Song, E. Alves, I. Bessa, E. Manino, L. Cordeiro *et al.*, “Verifying quantized neural networks using smt-based model checking,” *arXiv preprint arXiv:2106.05997*, 2021.
- [17] A. Lomuscio and L. Maganti, “An approach to reachability analysis for feed-forward relu neural networks,” *arXiv preprint arXiv:1706.07351*, 2017.
- [18] V. Tjeng, K. Xiao, and R. Tedrake, “Evaluating robustness of neural networks with mixed integer programming,” *arXiv preprint arXiv:1711.07356*, 2017.
- [19] M. Fischetti and J. Jo, “Deep neural networks and mixed integer linear optimization,” *Constraints*, vol. 23, no. 3, pp. 296–309, 2018.
- [20] R. Ivanov, J. Weimer, R. Alur, G. J. Pappas, and I. Lee, “Verisig: verifying safety properties of hybrid systems with neural network controllers,” in *Proceedings of the 22nd ACM International Conference on Hybrid Systems: Computation and Control*, 2019, pp. 169–178.
- [21] R. Ivanov, T. Carpenter, J. Weimer, R. Alur, G. Pappas, and I. Lee, “Verisig 2.0: Verification of neural network controllers using taylor model preconditioning,” in *International Conference on Computer Aided Verification*. Springer, 2021, pp. 249–262.
- [22] H.-D. Tran, X. Yang, D. M. Lopez, P. Musau, L. V. Nguyen, W. Xiang, S. Bak, and T. T. Johnson, “Nnv: The neural network verification tool for deep neural networks and learning-enabled cyber-physical systems,” in *International Conference on Computer Aided Verification*. Springer, 2020, pp. 3–17.
- [23] J. A. Vincent and M. Schwager, “Reachable polyhedral marching (rpm): A safety verification algorithm for robotic systems with deep neural network components,” *arXiv preprint arXiv:2011.11609*, 2020.
- [24] W. Xiang, H.-D. Tran, and T. T. Johnson, “Reachable set computation and safety verification for neural networks with relu activations,” *arXiv preprint arXiv:1712.08163*, 2017.
- [25] —, “Output reachable set estimation and verification for multilayer neural networks,” *IEEE transactions on neural networks and learning systems*, vol. 29, no. 11, pp. 5777–5783, 2018.
- [26] M. Everett, “Neural network verification in control,” *arXiv preprint arXiv:2110.01388*, 2021.
- [27] M. Mirman, T. Gehr, and M. Vechev, “Differentiable abstract interpretation for provably robust neural networks,” in *International Conference on Machine Learning*. PMLR, 2018, pp. 3578–3586.
- [28] T. Gehr, M. Mirman, D. Drachler-Cohen, P. Tsankov, S. Chaudhuri, and M. Vechev, “Ai2: Safety and robustness certification of neural networks with abstract interpretation,” in *2018 IEEE Symposium on Security and Privacy (SP)*. IEEE, 2018, pp. 3–18.
- [29] G. Singh, T. Gehr, M. Püschel, and M. Vechev, “An abstract domain for certifying neural networks,” *Proceedings of the ACM on Programming Languages*, vol. 3, no. POPL, pp. 1–30, 2019.
- [30] S. Bak, H.-D. Tran, K. Hobbs, and T. T. Johnson, “Improved geometric path enumeration for verifying relu neural networks,” in *International Conference on Computer Aided Verification*. Springer, 2020, pp. 66–96.
- [31] S. Chen, E. Wong, J. Z. Kolter, and M. Fazlyab, “DeepSplit: Scalable verification of deep neural networks via operator splitting,” *arXiv preprint arXiv:2106.09117*, 2021.
- [32] E. Wong and Z. Kolter, “Provable defenses against adversarial examples via the convex outer adversarial polytope,” in *International Conference on Machine Learning*. PMLR, 2018, pp. 5286–5295.
- [33] S. Boyd, N. Parikh, and E. Chu, *Distributed optimization and statistical learning via the alternating direction method of multipliers*. Now Publishers Inc, 2011.
- [34] S. Wang, H. Zhang, K. Xu, X. Lin, S. Jana, C.-J. Hsieh, and J. Z. Kolter, “Beta-CROWN: Efficient bound propagation with per-neuron split constraints for complete and incomplete neural network verification,” *Advances in Neural Information Processing Systems*, vol. 34, 2021.
- [35] K. Dvijotham, R. Stanforth, S. Goyal, T. A. Mann, and P. Kohli, “A dual approach to scalable verification of deep networks,” in *UAI*, vol. 1, no. 2, 2018, p. 3.
- [36] M. Fazlyab, M. Morari, and G. J. Pappas, “An introduction to neural network analysis via semidefinite programming,” in *2021 60th IEEE Conference on Decision and Control (CDC)*. IEEE, 2021, pp. 6341–6350.
- [37] A. Raghunathan, J. Steinhardt, and P. Liang, “Semidefinite relaxations for certifying robustness to adversarial examples,” *arXiv preprint arXiv:1811.01057*, 2018.
- [38] Y. Zheng and G. Fantuzzi, “Sum-of-squares chordal decomposition of polynomial matrix inequalities,” *Mathematical Programming*, pp. 1–38, 2021.
- [39] Y. Zheng, G. Fantuzzi, A. Papachristodoulou, P. Goulart, and A. Wynn, “Fast admm for semidefinite programs with chordal sparsity,” in *2017 American Control Conference (ACC)*. IEEE, 2017, pp. 3335–3340.
- [40] R. P. Mason and A. Papachristodoulou, “Chordal sparsity, decomposing sdps and the lyapunov equation,” in *2014 American Control Conference*. IEEE, 2014, pp. 531–537.
- [41] L. P. Ihlenfeld and G. H. Oliveira, “A faster passivity enforcement method via chordal sparsity,” *Electric Power Systems Research*, vol. 204, p. 107706, 2022.
- [42] H. Chen, H.-T. D. Liu, A. Jacobson, and D. I. Levin, “Chordal decomposition for spectral coarsening,” *arXiv preprint arXiv:2009.02294*, 2020.
- [43] B. Batten, P. Kouvaros, A. Lomuscio, and Y. Zheng, “Efficient neural network verification via layer-based semidefinite relaxations and linear cuts,” in *International Joint Conference on Artificial Intelligence (IJCAI21)*, 2021, pp. 2184–2190.
- [44] J. Lan, A. Lomuscio, and Y. Zheng, “Tight neural network verification via semidefinite relaxations and linear reformulations,” in *Proceedings of the 36th AAAI Conference on Artificial Intelligence (AAAI22)*, 2021.
- [45] T. Chen, J. B. Lasserre, V. Magron, and E. Pauwels, “Semialgebraic optimization for lipschitz constants of relu networks,” *Advances in Neural Information Processing Systems*, vol. 33, pp. 19 189–19 200, 2020.

- [46] R. A. Brown, E. Schmerling, N. Azizan, and M. Pavone, “A unified view of sdp-based neural network verification through completely positive programming,” in *International Conference on Artificial Intelligence and Statistics*. PMLR, 2022, pp. 9334–9355.
- [47] M. Newton and A. Papachristodoulou, “Neural network verification using polynomial optimisation,” in *2021 60th IEEE Conference on Decision and Control (CDC)*. IEEE, 2021, pp. 5092–5097.
- [48] —, “Sparse polynomial optimisation for neural network verification,” *arXiv preprint arXiv:2202.02241*, 2022.
- [49] A. Griewank and P. L. Toint, “On the existence of convex decompositions of partially separable functions,” *Mathematical Programming*, vol. 28, no. 1, pp. 25–49, 1984.
- [50] J. Lofberg, “Pre- and post-processing sum-of-squares programs in practice,” *IEEE transactions on automatic control*, vol. 54, no. 5, pp. 1007–1011, 2009.
- [51] K. Xu, Z. Shi, H. Zhang, Y. Wang, K.-W. Chang, M. Huang, B. Kailkhura, X. Lin, and C.-J. Hsieh, “Automatic perturbation analysis for scalable certified robustness and beyond,” *Advances in Neural Information Processing Systems*, vol. 33, pp. 1129–1141, 2020.
- [52] M. Fazlyab, M. Morari, and G. J. Pappas, “Probabilistic verification and reachability analysis of neural networks via semidefinite programming,” in *2019 IEEE 58th Conference on Decision and Control (CDC)*. IEEE, 2019, pp. 2726–2731.
- [53] A. Xue, L. Lindemann, A. Robey, H. Hassani, G. J. Pappas, and R. Alur, “Chordal sparsity for lipschitz constant estimation of deep neural networks,” *arXiv preprint arXiv:2204.00846*, 2022.